Металлофиз. новейшие технол. / Metallofiz. Noveishie Tekhnol.
2000, т. 22, № 5, с. 33—41

УДК 548.731

PACS numbers: 61.10.Lx, 61.66.Bi, 61.72.Dd, 61.72.Tt

D. Grigoriev, S. Manninen*, L. Datsenko, V. Khrupa, V. Molodkin, S. Galambosi*, V. Klad'ko, V. Machulin**

Institute of Semiconductor Physics, N.A.S.U.,
45 Prospekt Nauki, UA-03028 Kyyiv, Ukraine

*Department of Physics, University of Helsinki,
P.O.Box 9, Fin 00014, University of Helsinki, Finland

**G. V. Kurdyumov Institute for Metal Physics, N.A.S.U.,
36 AcademicianVernadsky Blvd., UA-03680 Kyyiv-142, Ukraine

ENERGY-DISPERSIVE STUDIES OF THE INTEGRATED REFLECTIVITY OF BRAGG DIFFRACTED CONTINUOUS X-RAY SPECTRUM FOR HIGH-SENSITIVE STRUCTURE DIAGNOSTICS OF IMPERFECT SINGLE CRYSTAL

The standard-free energy-dispersive method for investigation of the integral reflectivity as well as for determination of structure perfection parameter, i.e. static Debye—Waller factor of a real single crystal (with structure defects) for a wide range of wavelengths of X-ray continuous spectrum, is developed for the Bragg case of diffraction. Two Czochralski-grown silicon crystals with different levels of structure perfection are tested using this approach. The method happened to be very sensitive to structure distortions in the wavelengths shorter than 0.3 Å. Extending the range of the used wavelength to 0.2 Å provides more than one-order enhancement of the sensitivity and accuracy of the static Debye—Waller factor determination. The experimental results for reflectivities are found to be in a good agreement with predictions of the dynamical theory of X-ray scattering for crystals with homogeneously distributed structural defects. The application of the proposed method seems to be very promising for synchrotron-radiation sources.

Запропоновано безеталонний метод вимірювання інтегральної відбивної здатності (ІВЗ) реальних (які містять дефекти структури) монокристалів, а також інтегрального параметра структурної досконалості — статичного фактора Дебая—Валлера, що може бути застосований до широкого діапазону довжин хвиль рентгенівського випромінювання. Досліджувалися бездислокаційні монокристали кремнію, вирощені за методом Чохральського, що характеризувались різним рівнем структурної недосконалості. Метод виявився особливо чутливим до дефектів кристалічної гратки при використанні жорсткого рентгенівського випромінювання з довжиною хвилі меншою за 0,3 Å. Застосування запропонованого методу на довжинах хвиль РВ 0,2 Å дозволило більш як на порядок підвищити чутливість ІВЗ до структурних недосконалостей. Одержані експериментальні значення ІВЗ знаходяться у добрій згоді з передбаченнями динамічної теорії розсіяння рентгенівських променів на кристалах з однорідно розподіленими дефектами. Переваги запропонованого методу стають найбільш виразними при застосуванні синхротронних джерел рентгенівського випромінювання.

Предложен безэталонный энергодисперсионный метод измерения брэгговской интегральной отражающей способности (ИОС) реальных (содержащих дефекты структуры) монокристаллов, а также определения интегрального параметра структурного совершенства — статического фактора Дебая—Валлера, применимый в широком диапазоне длин волн рентгеновского излучения. Исследовались бездислокационные кристаллы кремния, выращенные методом Чохральского, характеризующиеся различным уровнем структурных искажений. Метод оказался особенно чувствительным к дефектам кристаллической решетки при использовании жесткого рентгеновского излучения с длиной волны меньшей 0,3 Å. Использование предложенного подхода на длинах волн РЛ 0,2 Å позволило более чем на порядок повысить чувствительность ИОС к структурным искажениям. Полученные экспериментально значения ИОС оказались в хорошем согласии с предсказанием динамической теории рассеяния рентгеновских лучей на кристаллах с однородно распределенными дефектами. Метод представляется особенно перспективным при использовании синхротронных источников рентгеновского излучения.

Key words: *integral reflectivity of single crystals, defects, dynamical theory of scattering, X-rays, diffractometry.*

1. Introduction

Integral reflectivity (IR) of a real (imperfect) crystal in the Bragg case of diffraction of X-rays (reflection geometry) is shown [1–6] to be highly sensitive, under certain conditions, not only to surface distortions, but to the volume structure distortions too. Comparing to the Laue case of diffraction (transmission geometry) Bragg one has various advantages, for instance: considerably higher diffraction maxima intensity, independence on thickness of massive samples, and opportunity of direct investigation of the diffuse component of scattering by the analysis of the spatial intensity distribution of the diffracted beam [2–4] in the single crystal scheme.

The IR sensitivity to structure distortions of the real crystals being characterized hereafter as the ratio $S = R_i/R_i^P$ (R_i, R_i^P stands for IR of imperfect and ideal crystals respectively), is known to increase while the X-ray wavelength λ decreases within the range $\lambda = 0.1–2$ Å. So the hard X-ray radiation is preferential for gaining a high reliability of the IR diagnostic method. On the other hand, one has to use rather soft X-ray radiation $\lambda = 0.9–1.5$ Å for the purpose of anomalous scattering effects investigation near the *K*-edges of the absorption for the atomic elements of such binary compounds as GaAs, GaP, GaN, *etc.*

The commonly accepted procedure for IR measurements by the double crystal spectrometer includes some basic problems. First of all, an extremely high supply voltage to excite intense hard characteristic lines (usually much more 100 kV) and rather complicated multicomponent monochromator are needed. Discrete set of the available characteristic lines offers a very limited possibility to study the energetic (spectral) dependencies of the IR, especially when the sharp peculiarities of the IR behaviour take place.

Single crystal diffraction scheme provides a relatively good possibility of the IR measurements for any λ using the continuous white beam spectrum of X-rays [7]. In this case however a reference sample (standard) with the known or predictable R_i value is necessary. Moreover, a special measurement should be made to separate the contribution of the apart X-ray long- and short-wave harmonics of used λ as well as the contribution of the inelastic scattering to the total intensity. The energy-sensitive detectors of X-ray radiation could serve to resolve this problem by the simplest way [8–10] as well as to register reflections of the different orders at a given Bragg angle θ_B simultaneously. Therefore the time of the carrying out an experiment may be considerably reduced.

An essential disadvantages of the X-ray tube comparing to synchrotron sources are obvious: less brilliance, restricted X-ray range with a considerably unsmooth energy white-beam spectrum overlapped by the sharp characteristic lines. Nevertheless, X-ray tubes are still the most widespread sources of radiation.

The main goal of the present work was to develop a quantitative method for the non-destructive defect structure diagnostics of the single crystals by means of the standard-free energy- dispersive IR measurements in the Bragg case of diffraction using continuous X-ray spectrum and single-crystal spectrometer.

2. Theoretical Background

The integrated intensity of X-rays, $I(E)$, scattered by a single crystal characterized by an IR, $R_i(E)$, could be written in the following way:

$$I(E) = R_i(E)J_0(E), \qquad (1)$$

where $J_0(E)$ is the intensity (per the unit solid angle) of the incident radiation with given energy E. Here we assume that the $J_0(E)$ value is the same within the angular range Ω of the incident beam and Ω exceeds the angular range of diffraction. Relation (1) permits to determine R_i values for the chosen imperfect single crystal directly from the $I(E)$, $J_0(E)$ values [8, 9]. To evaluate $J_0(E)$ dependence from the diffraction data a reference sample is needed first. Moreover it should have a perfect structure for using the dynamical theory of an ideal crystal to calculate its R_i value and in this way to avoid an ambiguity in $J_0(E)$ values.

It is well known [11–15] the X-ray scattering by real single crystals, such as industrially grown

Si, Ge, GaAs, GaP, GaN, *etc.* can be described by the dynamical diffraction theory [11–15]. In the framework of the theory developed for a crystal with homogeneously distributed defects [13–15] the following expression for the R_i have been obtained:

$$R_i = R_i^B + R_i^D =$$

$$= R_i^{dyn} P(\mu_0, \mu_{ds}^0, t) e^{-L} + R_i^{kin} \Pi(\mu_0, \mu^*, t)(1 - e^{-2L}), \quad (2)$$

where R_i^B, R_i^D stand for coherent and diffuse component of scattering respectively, R_i^{dyn}, R_i^{kin} correspond to IR values of a perfect and ideally-mosaic crystal. Expression (2) involves integral parameters of structure perfection *i.e.* the static Debye–Waller factor L and extinction coefficients of the additional energy losses due to the diffuse scattering on defects μ_{ds}^0, μ^* for coherent, R_i^B, and diffuse, R_i^D components respectively apart of the photoelectric absorption described by the μ_0 coefficient. The generalized Prince factor $P(\mu_0, \mu_{ds}^0, t)$, takes into account both μ_0 and μ_{ds}^0 absorption coefficients that effect the R_i^B values. $\Pi(\mu_0, \mu^*, t)$ takes into the account the absorption level $(\mu_0 + \mu^*)t$ for the diffusely scattered waves in a finite sample.

For interpretation of the experimental $R_i(\lambda)$ data both the advanced theory [15] and its simplified form [14] were used. Let us restrict ourselves here by the relevant expressions according to [14]:

$$R_i^{dyn} = \frac{16}{3\pi} \frac{CQ\Lambda}{\gamma_0}, \quad R_i^{kin} = C^2 Qt/\gamma_0, \quad (3)$$

$$\Pi(\mu_0, \mu^*, t) \cong \begin{cases} \dfrac{1}{[2(\mu_0 + \mu^*)t/\gamma_0]}, & \text{if } \mu_0 t >> 1 \\ \dfrac{1}{[1 + (\mu_0 + \mu^*)t/\gamma_0]}, & \text{if } \mu_0 t << 1,\ t >> \Lambda \end{cases}$$

$$P(\mu_0, \mu_{ds}^0, t) \cong 1 - 3\frac{\pi}{4} \frac{(\mu_0 + \mu_{ds}^0)\Lambda}{C\gamma},$$

where

$$1/\gamma = \frac{1/\gamma_0 + 1/\gamma_h}{2};$$

$Q = (\pi|\chi_{hr}|)^2/\lambda\sin(2\theta)$ is the kinematical reflectivity related to the unit length. Finally

$$\Lambda = \lambda\sqrt{\gamma|\gamma_h|}/2\pi|\chi_{hr}|$$

is the extinction length for a chosen reflection *hkl*.

Necessary relations between the most important parameters of the Coulomb-type defects (characteristic size r_{cl} and concentration n) and diffraction parameters L, μ_{ds}^0 and μ^* should be also given:

$$\mu^* = \frac{2\mu_{ds}^0}{(1 - 1/\alpha)\ln\alpha}\left(\frac{A}{D} - \frac{\ln\alpha}{\alpha} - \frac{F}{D}\frac{1}{\alpha}\right), \quad (4)$$

$$L = \frac{2\mu_{ds}^0 \Lambda}{\pi\gamma_0|\gamma_h|} D(\alpha - 1)/\ln\alpha, \quad (5)$$

$$\mu_{ds}^0 = m_0 B \ln\alpha, \quad (6)$$

where

$$\alpha = \Lambda/r_{cl},$$

$$A = 1 + a(8/9) + a^2(4/15),$$

$$D = 1 + a(2/3), \quad F = 1 + a + a^2(2/5),$$

$$\beta = (3\nu^2 + 6\nu - 1)/4(1 - \nu^2),$$

$$m_0 = \pi nb(C\chi_h h/2n)^2, \quad B = 2B_1 + B_2\cos^2\theta;$$

for clusters: $a = \mathrm{tg}^2\theta - 0.5$, $B_1 = 0$, $B_2 = (4\pi A_{cl}/\nu)^2$; for loops: $a = (\mathrm{tg}^2\theta - 0.5)/(1 + 2/\beta\cos^2\theta)$, $B_1 = 4(b\pi r_{cl}^2/\nu)^2/15$, $B_2 = \beta B_1$.

In these formulas C, γ_0, γ_h stand for the polarization factor, the directional cosines respectively, χ_{hr} is the real part of the h-th Fourier component of the crystal susceptibility, t, h, ν, ν, b are respectively the thickness, the diffraction vector, the unit-cell volume, the Poisson ratio, the Burgers-vector magnitude. A_{cl} is the constant of so-called power of Coulomb defect [16]. It depends on the volume change ΔV of a crystal due to appearing of defect as well as on the Poisson ratio ν.

Note, while the parameter L characterizes the statistically averaged distortion level due to defects for the acting diffraction vector h, the parameter r_{cl} in (4)–(6) is rather the characteristic of the local distortion field caused by the individual defect of the type predominated in a scattering volume. Thus, the deformation field for the Coulomb-type defects at the relative position r can be written as $U(\mathbf{r}) = A_{cl}\frac{\mathbf{r}}{|\mathbf{r}|^3} = \varepsilon r_{cl}^3 \frac{\mathbf{r}}{|\mathbf{r}|^3}$, where ε is the dimensionless constant. r_{cl} is assumed to be independent on the diffraction conditions at the first approximation. However the averaged size of the incoherently scattering region r_d depends considerably on the wavelength λ as well as on h and may be

related to r_{cl} in the following way $r_d = r_{cl}(\varepsilon H \mathrm{tg}\theta)^{1/2}$ [18]. Ratio $\alpha = \Lambda/r_{cl}$ determines the extent of the extinction processes in the diffuse scattering that are implemented in (2) through the terms μ_{ds}^0 and μ^*. So, each of the parameters L, r_{cl} represents the different properties of the deformation field. They are independent on the X-ray wavelength and the pair of these parameters describes quantitatively the curve $R_i(\lambda)$. in an unique way according the expressions (2)–(6). This is why the parameters L and r_{cl} where chosen as a key role when the experimental values of $R_i(\lambda)$ have been fitted by the theoretical ones and analysed, despite the fact that in the commonly accepted approach parameters L, μ_{ds}^0 and μ^* are usually used as the basis.

3. Experimental

Experiments were carried out in the University of Helsinki, X-ray Laboratory. Two different X-ray sources: tungsten anode tube under supply voltage 100 kV and silver anode tube, 30 kV correspondingly were used. This circumstance provided essentially different character of energetic spectra of the incident beam. Energy-dispersive Ge solid state detector and multi-channel analyser (2048 channels) were used. Radioactive ^{241}Am source was used for the calibration of the energy scale.

Single crystal spectrometer was very similar to the classical one except some details in the collimator unit. Two pairs (horizontal and vertical) of the adjustable tungsten slits, separated by a distance of 20 cm, were used for collimation of the incident beam. This provided a narrow square beam of 0.02 cm^2 at the sample position. The slits were made from a heavy element (tungsten), so that the undesired contribution of the secondary fluorescent radiation caused by the slits into the final spectra was sufficiently minimized.

Because all the X-ray intensity of a beam, reflected by the single crystal sample should be gathered to obtain reliable values of R_i, the spatial deviation of the reflected beams wasn't restricted. Under these conditions the mosaic-crystal reference sample used in [9, 10] was inefficient to determine the energy spectra of the incident beam. Taking into account the certain imperfection of the available single crystals for a reference samples we were enforced to derive $I_0(E)$ dependence directly by means of the energy-dispersive detector positioned at the direct beam. No absorbing foils were used in order to preserve the original spectral distribution $I_0(E)$. The total flux was minimized by the slits to limit the dead time of the detector (less then 2%) during the measurements.

An exact Bragg set (θ for the sample and 2θ for the detector) was obtained using the sharp characteristic components of the spectra (L series for tungsten tube and K-series for silver one. The desired wavelength λ was varied by the simultaneous rotation $\Delta\theta/\Delta 2\theta$ of the sample and the detector correspondingly.

Two dislocation-free Czochralski-grown silicon crystals were chosen for the experiment, first in its as-grown state, the second sample was annealed (1100°C for 6.5 h). Thickness of the given samples (1 cm for sample 1, 1.5 cm for sample 2) was enough to consider by calculation the samples as semi-infinite ones in all the range of λ. The crystals were chemically etched in order to remove possible strains from the surfaces (111).

The integral intensities $I_R(E)$ of a reflected beam within the range of $\lambda = 0.25$–1.4 Å for the reflections (111) and (333) as well as the spectral distribution of the incident beams for the every experiment were analysed.

Reference values of the R_i for the samples under investigation were measured using a standard double-crystal spectrometer (Mo$K_{\alpha 1}$-radiation) for (111) and (333) reflections.

4. Results and Discussion

A typical energy spectrum of the diffracted beam $I_R(E)$ ($\theta_B = 9.64°$, $\lambda = 0.35$ Å for (333) reflection) obtained by the energy-dispersive detector in the case of the W-tube source is represented at Fig. 1, *a* to illustrate some common features and effects that are present when the intensity is being registered by the energy-sensitive detector. Besides the destined Bragg peaks marked by their indices 111–555 some additional peaks could be observed. Elastic and Compton peaks caused by the strong characteristic WK_α and WK_β lines are marked as C_K. The escape peaks (E marks) due to the escape of Ge-fluorescence photon from the

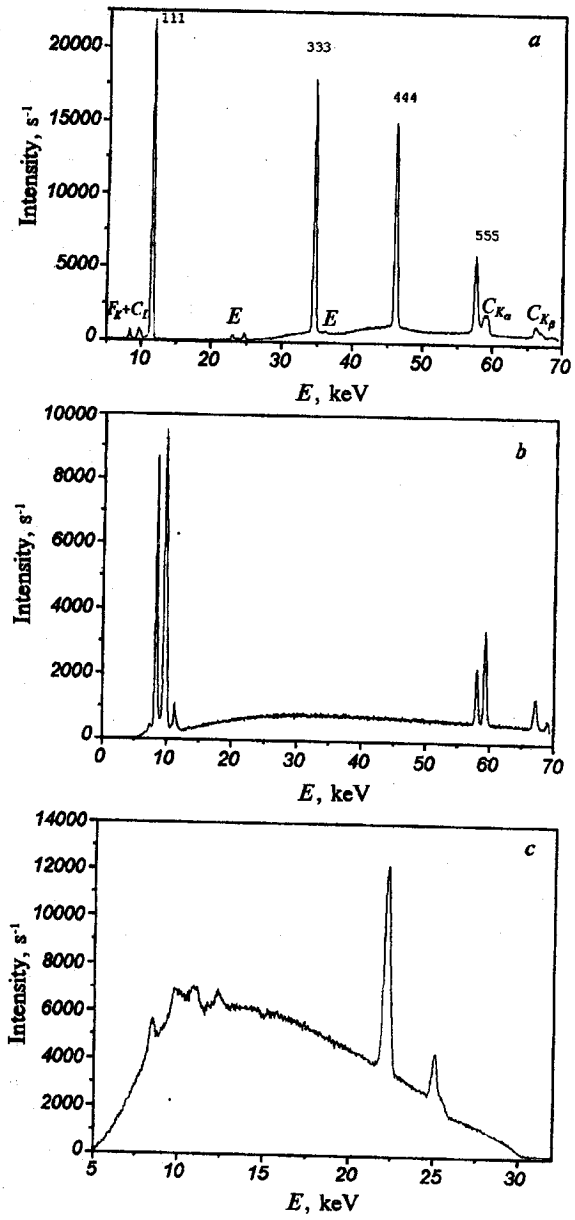

Fig. 1. Experimental energy spectra measured by an energy-dispersive Ge detector: *a*—diffracted by a single Si crystal, W-tube, $\theta_B = 9.64°$, $\lambda = 0.35$ Å for (333) reflection; *b*—incident beam, tungsten anode, $U = 100$ keV; *c*—incident beam, silver anode, $U = 30$ keV.

Ge detector, shifted down by the Ge *K*-shell fluorescence energies (approx. 10 keV) from the original energies of the diffraction peaks as well as the fluorescent *K*-lines of the Ge (F_k marks) occur at the final spectrum. Inelastic scattering provides also a continuos background observed clearly at the energy range of 25–70 keV.

Escape peak intensities should be taken into the account when the integrated intensity of the diffracted beam is calculated. The whole set of the experimental energy dependences $I_R(E)$ for the different E permitted us to find experimentally the dependence between the integrated intensities of the main (Bragg) and escape peaks. Using this dependence the spectral distribution of the intensity of the incident beam was separated from the contribution of the escape component.

The resulting incident beam spectra are represented at Fig. 1, *b*, *c* for the tungsten and silver tubes. One should note that the shown intensities do not correspond the real brightness of the tubes because a tight collimation was used. Having much higher voltage supply for W tube we got strong and sharp characteristic *K* and *L* lines produced by the target and comparatively smooth energetic distribution of the white-beam spectra within the range 20–70 keV. In case of silver tube, referring to the not so high excitation of the target (30 kV were supplied) we could consequently observe the comparatively low intense characteristic Ag*K*-lines. Some small additional peaks caused by the fluorescence within the detector are located close to 10 keV.

The dependences of the relative reflectivities

$$R_E(E) = \int \frac{I_R(E)}{I_0(E)} dE = \int \frac{I^m(E) + I^e(E)}{I_0(E)} dE$$

for the chosen crystals (here $I^m(E)$, $I^e(E)$, $I_0(E)$ stand for the elastic, escape and incident beam partial intensities respectively) are represented at Fig. 2, *a*, *b* for the reflections 111 and 333 correspondingly. Index E in $R_E(E)$ means that integration is being carried out over the energy near the elastic reflection peak. The program for integration subtracts the background automatically.

As it is seen from Fig. 2, the R_E values for both of the given samples differ for both reflections slightly in the soft X-ray region ($\lambda > 0.6$ Å). For harder radiation ($\lambda < 0.4$ Å) the R_E magnitudes as well as the differences between them obtained for as-grown silicon crystal and annealed one sufficiently grow. The R_E values for the boundary wavelengths used in the experiment ($\lambda = 0.2$ Å, 62 keV and $\lambda = 1.2$ Å, 10.325 keV) as well as their ratios $R_E(0.2)/R_E(1.2)$ are collected in the Table 1. Last ratios were given to illustrate numerically the

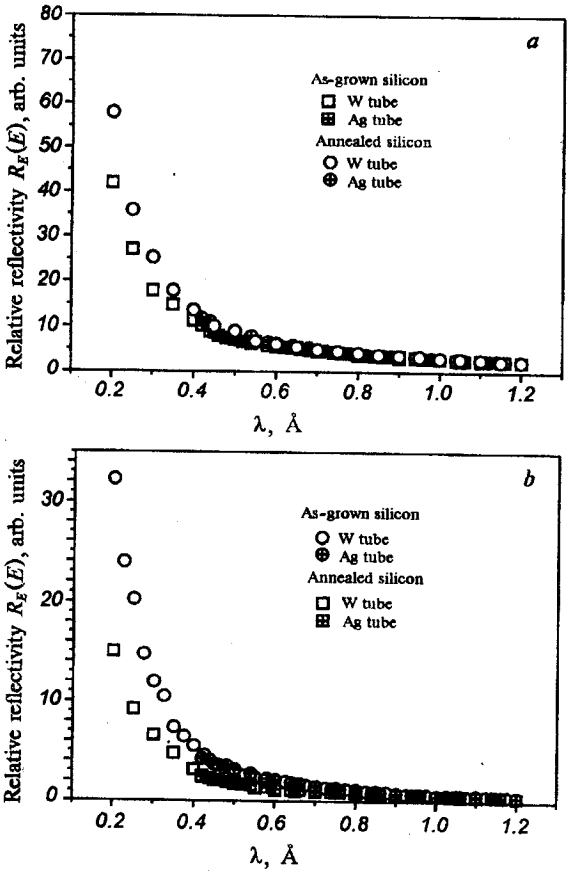

Fig. 2. Dependences of the relative reflectivities $R_E(E) = \int I_R(E)/I_0(E)dE$ for 111 (*a*) and 333 (*b*) reflections of the X-ray wavelength λ.

fact, that the sensitivity of the relative integrated intensity values R_E, derived in the energy-dispersive diffraction experiments, to structure defects as well as the signal-background ratio are increasing considerably in the short wavelength region.

To find the values of an integral reflectivity in its traditional meaning (see the expression (2)), the experimental $I(E)/I_0(E)$ dependences should be integrated over the λ scale at the reflection peaks. Integral reflectivities obtained in this way are expressed in arbitrary units. They differ from the real IR values only by the normalizing constant. This normalization have been performed using the Mo$K_{\alpha 1}$ double crystal spectrometer. Reference IR values are given in Table 2.

The experimental dependences $R_i(\lambda)$ recalculated in real values are presented at Fig. 3, *a*, *b* for the 111 and 333 reflections correspondingly. In a contrast with the dependences represented at Fig. 2, the curves $R_i(\lambda)$ demonstrate now a non-monotone behaviour, with a some minima at $\lambda = 0.4$–0.5 Å which are seen more distinctly for the 333 reflection. Towards shorter X-ray wavelengths the steep growth of R_i values as well as their difference for the different samples could be observed. These phenomena are caused by the growing contribution of the diffusely scattered beams while λ is decreasing. At the same time, for the range $\lambda > 0.6$ Å, which is more common for the ordinary tubes, the dependences $R_i(\lambda)$ seem to be linear and the values of R_i close to each other for different samples and approaching to the dynamic limits R_i^P. Small values of $R_i - R_i^P$ (the key parameter for evaluation of imperfection level in diagnostics methods based on IR measurements) convinces us once more the known small sensitivity of soft X-ray radiation to structural defects.

Theoretical dependences $R_i(\lambda)$ were fitted to the experimental data using two key parameters of distortion level mentioned above, r_{cl} and L. The behaviour of the theoretical $R_i(\lambda)$ curves was found to be strongly sensitive to the Debye–Waller factor L values in short-wave range, being almost independent on the characteristic radii r_{cl}. In other words, so-called one-parameter approximation [3, 17] takes place here. Debye–Waller factor L values calculated from the $\lambda < 0.4$ Å region data are represented at the Table 3. These values are common for all the discussed curve.

Table 1. **Relative integrated intensities R_E for λ = 0.2 and 1.2 Å and their ratios for the samples under investigation in arbitrary units (111 and 333 reflections).**

Sample	Reflection					
	111			333		
	R_E(1.2 Å)	R_E(0.2 Å)	R_E(0.2 Å)/R_E(1.2 Å)	R_E(1.2 Å)	R_E(0.2 Å)	R_E(0.2 Å)/R_E(1.2 Å)
As-grown	2.4	25	10.4	0.52	15	28.85
Annealed	2.6	38.24	14.7	0.56	32.2	57.5

Table 2. Reference R_i values measured by the double-crystal technique (MoK_{α_1}-radiation, λ = 0.71 Å).

Sample	Reflection	
	111	333
As-grown	$2.31 \cdot 10^{-5}$	$5 \cdot 10^{-6}$
Annealed	$2.55 \cdot 10^{-5}$	$6.9 \cdot 10^{-6}$

Table 3. Experimental Debye–Waller factor L values obtained by the fitting.

Sample	Reflection	
	111	333
As-grown	$3 \cdot 10^{-3}$	$1.5 \cdot 10^{-2}$
Annealed	$6 \cdot 10^{-3}$	$3.2 \cdot 10^{-2}$

One should draw attention, that the ratios $L_{333}/L_{111} \sim 5$ for both of crystals correspond well the dependence $L \sim h^{3/2}$ which is valid for a model of small dislocation loops [16].

It was found for the soft X-ray range ($\lambda > 0.6$ Å) that the sensitivity of the $R_i(\lambda)$ curve to r_{cl} parameter doesn't grow enough that one could determine r_{cl} with a high precision. So the fitting procedure gives r_{cl} values which are in the interval 0.1–5 μm. The main reason for this uncertainty is the Bragg geometry itself where the mean lengths of the diffuse wave traces from the origin point to the exit surface are comparable with the absorption length. While the experimental IR data even for the annealed sample are not considerably different from R_i^p values (as it could be seen in the soft-wave range) the dynamic effects in diffuse scattering (expressed by μ_{ds}^0 and μ^* terms of the formulas (2)–(6) that are dependent on r_{cl}) are correspondingly low.

Resuming, we should note, that small (0.1–5 μm) dislocations loops ($h^{3/2}$ dependence of L) are presented in the volume for both given crystals. Unfortunately, fifty times discrepancy in r_{cl} values doesn't allow us to calculate the concentration of the mentioned defects. To evaluate r_{cl} an additional independent experimental data should be involved [19].

Generally, the IR becomes more sensitive to the r_{cl} parameter under the higher imperfection

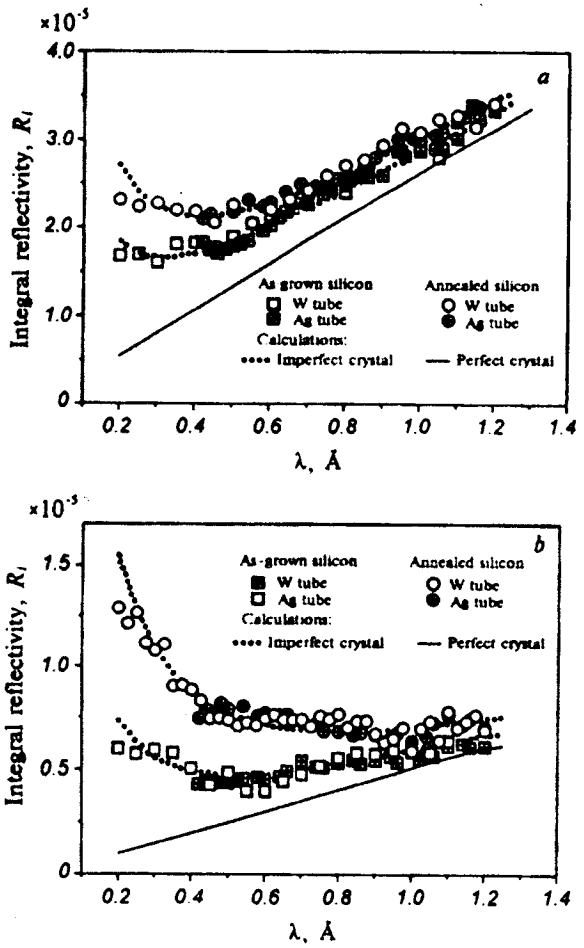

Fig. 3. Dependence of the integrated reflectivities R_i on the X-ray wavelength λ for 111 (*a*) and 333 (*b*) reflections.

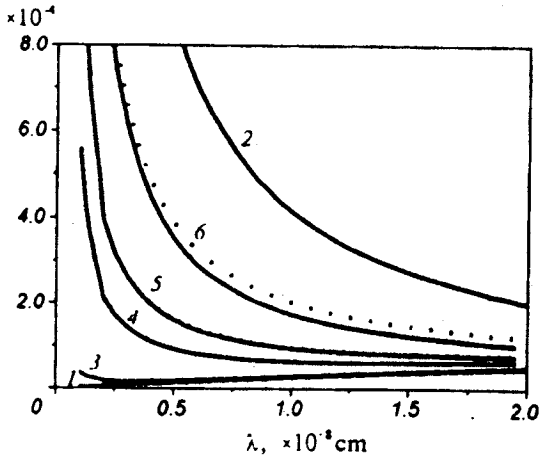

Fig. 4. The calculated dependences of the integrated reflectivities R_i on the X-ray wavelength λ calculated for silicon single crystals, reflection 111: perfect crystal (*1*), mosaic crystal (*2*) and for imperfect crystals with the following values of Debye–Waller factor $L = 3 \cdot 10^{-3}$ (*3*), $L = 1 \cdot 10^{-2}$ (*4*), $L = 5 \cdot 10^{-2}$ (*5*), $L = 2 \cdot 10^{-1}$ (*6*). For series 3–6 dotted and solid lines correspond to r_{cl} = 1 μm and r_{cl} = 10 μm, respectively.

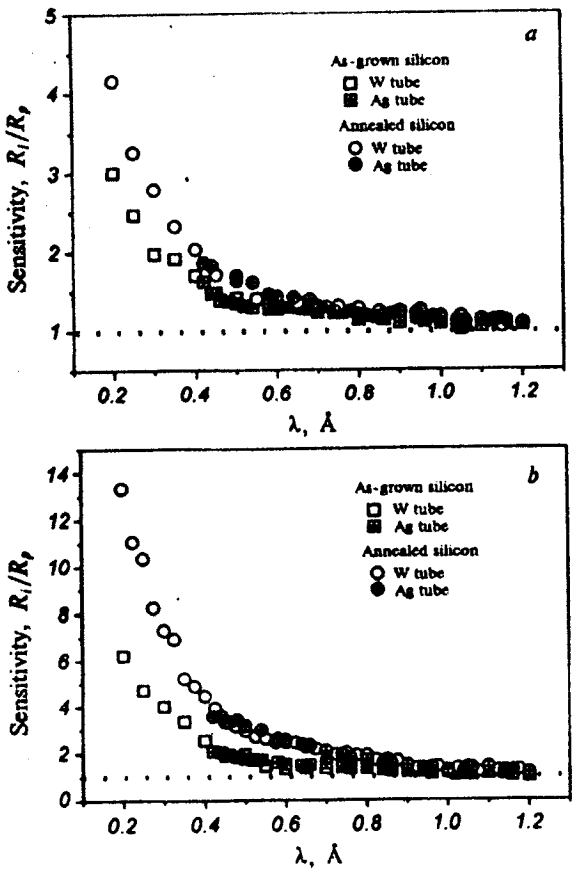

Fig. 5. The sensitivity of the integrated Bragg reflectivity R_i/R_p to the structure distortions versus λ for the 111 (*a*) and 333 (*b*) reflections.

level. To illustrate this fact, the calculated set of R_i for the different L values and the r_{ci} fixed at 1 and 10 μm levels are represented in Fig. 4. The noticeable splitting of the curve series calculated for given L and different r_{ci} became suitable for detection at $L = 0.1$ that exceeds the experimentally determined levels by two orders.

The applicability of the present method for the structure defect diagnostics could be illustrated in another way. The sensitivity of the IR to the structure defects has been signified here as the ratio $R_i(\lambda)/R_i^p(\lambda)$. As one can see from Fig. 5, *a*, *b* the ratio $R_i(\lambda)/R_i^p(\lambda)$ (the reflections 111 and 333 respectively) depends essentially on the reflection order as well as on the X-ray wavelength. More then ten times enhancement of $R_i(\lambda)/R_i^p(\lambda)$ ratio in the case of the investigated relatively perfect Si samples for $\lambda = 0.2$ Å and $\lambda = 1.2$ Å have been observed for 333 reflection. This ratio increases extremely sharp in the wavelength region $\lambda < 0.3$ Å.

5. Conclusion

Standard-free energy-dispersive method for measurements of the integral reflectivity for single crystals within a wide range of the X-ray wavelengths have been developed. Integral reflectivities of the silicon dislocation-free single crystals in as-grown state and annealed one in the Bragg case of diffraction were investigated using the proposed method. Integral structure perfection parameters L (Debye–Waller factor) for the given crystals were determined.

Considerable differences of the reflectivities of both samples were established experimentally on continuous X-ray spectra regardless the sources. The results are found to be in a good agreement with the theoretical predictions and demonstrate some specific features of the dynamical diffraction in the imperfect crystal:

⇒ Integrated reflectivity $R_i(\lambda)$ was shown to have a non-monotonous behaviour and could be explained by the specific effects in growing diffusely scattered component in the short-wave X-ray region.

⇒ The previously known high IR sensitivity to the defect level in the hard X-ray range was proved and found to increase strongly for X-ray wavelengths $\lambda < 0.3$ Å.

⇒ For the soft X-ray range it was proved that the IR values for the different samples decrease and become close to those calculated for the perfect crystal.

⇒ Extending the range of the used wavelength to 0.2 Å provides more than one order enhancement of the sensitivity and accuracy of the static Debye–Waller factor determination.

The application of the proposed method seems to be very promising for synchrotron radiation sources

Acknowledgements

The authors want to thank the Center for International Mobility (CIMO), Finland and the Academy of Finland for financial support.

1. *V. Holy* // Acta Crystallogr Sect A. — 1984. — **40**, No. 6. — P. 675.

2. *I. R. Entin, V. I. Khrupa* // J. Appl. Crystallogr. — 1991. — **24**, No. 4. — P. 403.

3. *V. I. Khrupa, S. M. Krasulya, L. I. Datsenko, V. F. Machulin* // Ukr. Fiz. Zh. — 1998. — **43**, No. 2. — P. 224.

4. *D. O. Grigoriev, V. I. Khrupa* // Metallofiz. Noveishie Tekhnol. — 1994. — **16**, No. 12. — P. 23.

5. *V. P. Klad'ko, D. O. Grigoriev, L. I. Datsenko et al.* // Semiconductor Physics, Quantum Electronics & Optoelectronics. — 1999. — **2**, No. 1. — P. 157.

6. *A. Freund* // SPIE Conf. on Advanced X-Ray-UV Radiation Sources and Applications. SPIE Proc. 1345. — 1990. — P. 234.

7. *L. I. Datsenko, A. N. Gureev, V. I. Khrupa et al.* USSR Patent N1255906 // Bulletin of Inventions. — 1986. — No. 33. — P. 168.

8. *T. Fukamashi, S. Hosoya, M. Okunuki* // Acta Crystallogr. Sect. A. — 1976. — **32**, No. 1. — P. 104.

9. *B. Buras, J. Staun Olsen* // J. Appl. Crystallogr. — 1977. — **10**. — P. 431.

10. *V. Honkimäki, P. Suortti* // J. Appl. Crystallogr. — 1992. — **25**. — P. 97.

11. *N. Kato* // Acta Crystallogr. Sect. A. — 1980. — **36**, No. 7. — P. 763.

12. *P. Dederichs* // Solid State Phys. — 1972. — **27**. — P. 135.

13. *L. I. Datsenko, V. B. Molodkin, M. E. Osinovskii.* Dynamical X-Ray Scattering by Real Crystals. — Kiev: Naukova Dumka, 1988.

14. *V. G. Bar'yakhtar, V. V. Nemoshkalenko, V. B. Molodkin et al.* // Metallofizika. — 1993. — **15**, No. 12. — P. 18.

15. *V. B. Molodkin, S. N. Olikhovsky, E. N. Kislovsky et al.* // Metallofiz. Noveishie Tekhnol. — 1997. — **19**, No. 12. — P. 25.

16. *P. Dederichs* // Phys. Rev. B. — 1970. — **1**, No. 4. — P. 1306.

17. *R. Schneider* // J. Appl. Crystallogr. — 1974. — **7**. — P. 547.

18. *A. I. Nizkova, A. N. Gureev, L. I. Datsenko* // Fiz. Tverd. Tela. — 1984. — **26**, No. 3. — P. 811.

19. *V. B. Molodkin, V. V. Nemoshkalenko, A. I. Nizkova et al.* // Preprint UNSC 1.1998. — Kyyiv, 1998.

Received 16.03.2000 (in final version — 25.04.2000)